Tubulin Structure Probed with Antibodies to Synthetic Peptides. Mapping of Three Major Types of Limited Proteolysis Fragments†

Sonsoles de la Viña,‡ David Andreu,§ Francisco Javier Medrano,‡ Juan Miguel Nieto,‡ and Jose Manuel Andreu*,‡

Centro de Investigaciones Biológicas, CSIC, Velazquez 144, 28006 Madrid, Spain, and Departamento de Quimica Organica, Universidad de Barcelona, Marti i Franquês 1, 08028 Barcelona, Spain

Received September 4, 1987; Revised Manuscript Received March 10, 1988

ABSTRACT: We synthesized five peptides homologous to the potentially antigenic positions α(214–226), α(430–443), α(415–443), β(241–256), and β(412–431) of the porcine brain tubulin sequences. These peptides were successfully employed to raise tubulin-cross-reactive antibodies. The antibodies are specific of the regions of tubulin spanned by the peptides. They react specifically with the tubulin bands in immunoblots and with microtubules in immunofluorescence assays of cytoskeletons. The peptides of the C-terminal regions have also been employed to localize determinants recognized by two available monoclonal antibodies to tubulin in the positions α(415–430) and β(412–431), respectively. In a first application of the anti-peptide antibodies, we have mapped the fragments of limited proteolysis of purified calf brain tubulin by trypsin, chymotrypsin, papain, thermolysin, subtilisin, and protease V8 from *Staphylococcus aureus*. Thirty-seven peptides have been identified, of which 32 have been unequivocally aligned into the tubulin sequences on the basis of their antigenic reactivity. There are three major, well-defined zones of preferential cleavage by the proteases: the C-termini and two internal zones in each chain. C-Terminal cleavages of both chains by subtilisin do not remove the antigenic reactivity of the zones α(415–430) and β(412–431). C-Terminal cleavages by protease V8 are preferential of β-tubulin. All six proteases tested cleave α- and/or β-tubulin at one or both of the internal zones. These zones are located roughly at one-third and two-thirds of the chain length in both subunits. Therefore, a model of the tubulin monomers is proposed which consists of three major, proteolytically defined, compact regions (N-terminal, middle, and C-terminal thirds) and the cleavable zones. This model is discussed with the tubulin structural information presently available.

The structure of microtubules is known from electron microscopy, image reconstruction, and X-ray diffraction studies (Amos, 1979; Mandelkow & Mandelkow, 1985; Mandelkow et al., 1977). In these studies the internal structure of the subunits, α- and β-tubulin, was scarcely detectable. On the other hand, the amino acid sequences of α- and β-tubulins from pig brain are known (Ponstingl et al., 1981; Krauhs et al., 1981) as well as the nucleotide sequences of a number of tubulin genes from different organisms (Valenzuela et al., 1981; Cleveland & Sullivan, 1985). Each tubulin isotype is strongly conserved in evolution and shows variable homology to the others. The physical properties of soluble tubulin, the α–β heterodimer, have been extensively characterized (Na, 1982; Lee, 1981). However, tubulin crystals suitable for high-resolution X-ray analysis have not been reported, and therefore the three-dimensional structure of this protein remains largely unknown. The secondary structure forming potentials of the tubulin sequences are generally low (Ponstingl et al., 1981). Although part of the tubulin molecule may be modeled on the basis of local homologies to other nucleotide binding proteins (Mandelkow et al., 1985b; Sternlicht et al., 1987), a wealth of information is still essentially hidden between the primary structure of the tubulin subunits and the structure of microtubules. This includes the folding of the polypeptide chains, their interactions to form the soluble heterodimer, the interactions among heterodimers in the microtubule wall, and the interactions with assembly-modifying ligands and microtubule-associated proteins. A variety of approaches to the structural and functional mapping of the tubulin molecule have been taken, such as the comparison of tubulins and tubulin mutants with different primary structures, affinity labeling of ligand binding sites, chemical modification and cross-linking, limited proteolysis, and specific antibodies (Soifer, 1986).

Limited proteolysis of tubulin has proven very useful, although conflicting and difficult to reproduce results have appeared in the literature. Maccioni and Seeds (1983) suggested that chymotrypsin cleaves both α- and β-tubulin at positions Phe-135 and Phe-133, respectively. However, Mandelkow et al. (1985a) have shown, by sequencing several N-terminal residues of the fragments, that chymotrypsin cleaves preferentially β-tubulin at Tyr-281, whereas trypsin cleaves preferentially α-tubulin at Arg-339. A model of the substructure of the tubulin molecule has been proposed in which each subunit is made of a large N-terminal domain (roughly two-thirds of the polypeptide chain, containing the GTP binding site) and a small C-terminal domain. Proteolytic nicking combined with chemical cross-linking has indicated that the N-terminal domain of α contacts the C-terminal domain of β in the tubulin heterodimer; the interaction between heterodimers along the protofilaments of microtubules should be between the small domain of α and the large domain of β (Kirchner & Mandelkow, 1985).

Preferential subtilisin cleavage of small fragments at the very acidic C-termini of α- and β-tubulin under particular conditions renders S-tubulin, which has an increased ability to polymerize without the participation of MAPs[1] (Serrano

† This work was supported in part by a grant from CAICyT to CSIC Project 184 (1985–87). A preliminary report was presented at the 10th American Peptide Symposium, St. Louis, MO, May 1987.

‡ Centro de Investigaciones Biológicas, CSIC.

§ Departamento de Quimica Organica, Universidad de Barcelona.

0006-2960/88/0427-5352$01.50/0

et al., 1984a). A molecular weight of 4000 was reported for the small subtilisin fragments responsible for MAPs binding (Serrano et al., 1984b). Serrano et al. (1986a) have quoted cleavage points at residues 411 and 417 in both subunits whereas Maccioni et al. (1986) have indicated the subtilisin cleavage sites to be at Glu-417 in α and Glu-407 in β. However, Sackett et al. (1985) concluded that subtilisin cleavages tubulin at sites between 7 and 15 residues from the C-terminal ones (that is, between α residues 436 and 444 and between β residues 430 and 438).

There is general agreement on the fact that the small C-terminal fragments of tubulin cleaved by subtilisin are spontaneously released from the protein. These regions are considered very flexible (Ponstingl et al., 1979; Ringel & Sternlicht, 1984) and exposed on the surface of microtubules (Breitling & Little, 1986). However, tubulin nicked by trypsin or chymotrypsin does not appear to dissociate into its fragments so easily, indicating substantial interactions between them. Kirchner and Mandelkow (1985) had to employ denaturing conditions to dissociate their fragments. Cysteine residues 239 and 354, distant in the sequence of β-tubulin and corresponding to different chymotryptic fragments, are cross-linked by *N*,*N*′-ethylenebis(iodoacetamide), indicating that they are maximally 9 Å apart in the tertiary structure (Little & Ludueña, 1985). Cys-12 and Cys-201 or -211 of β-tubulin also appear to be maximally 9 Å apart (Little & Ludueña, 1987). The region around position 239 of β-tubulin appears to be related to colchicine binding, since the reaction of the sulfhydryl cross-linker is inhibited by colchicine and its A ring analogues (Roach & Ludueña, 1985) and yeast tubulin, which binds colchicine weakly (Kilmartin, 1982), has Ser instead of Cys at position β-239 (Neff et al., 1983). Plant tubulin binds colchicine with low affinity (Morejohn et al., 1984), and algal β-tubulin has one of the major clusters of differences with respect to mammalian β-tubulin at positions 222, 229, 232, 236, and 238 (Youngbloom et al., 1984). It has also been reported, in contrast to the above, that the tryptic fragments of tubulin come apart in gel chromatography and the colchicine binding site is located in the small C-terminal tryptic fragment of α-tubulin (Serrano et al., 1984b; Avila et al., 1987). A careful photoaffinity labeling study has indicated that the colchicine site is located in the α subunit (Williams et al., 1985) or no more than 18 Å apart from it (Little & Ludueña, 1985).

Different antibodies of known specificity have been employed to study tubulin. Mandelkow et al. (1985a) succeeded in raising polyclonal antibodies to isolated α and β chains and separated the chain-specific from the cross-reacting antibodies. The monoclonal antibody YL 1/2 (Kilmartin et al., 1982) recognizes the tyrosinated C-terminus of α-tubulin and binds to the surface of microtubules in vitro and in microinjected cells (Wehland et al., 1983, 1984). Piperno and Fuller (1985) produced monoclonal antibodies that specifically recognize acetylated α-tubulin and employed them to localize this posttranslationally modified tubulin in axonemal microtubules from various organisms. Gundersen et al. (1984, 1987) raised two monospecific antibodies that react with the tyrosinated and nontyrosinated α C-terminus, respectively, and they have employed these antibodies to study the role of tyrosination in microtubule differentiation.

We reasoned that antibodies specific for relevant small antigenic sequences of tubulin would be valuable probes to study the structure and interactions of this protein. In this paper we report the selection of potentially antigenic regions, the properties of antibodies to tubulin synthetic positions α(214–226), α(415–443), α(430–443), β(241–256), and β-(412–431), and their use to unequivocally map fragments of limited proteolysis by trypsin, chymotrypsin, papain, thermolysin, V8 protease, and subtilisin into the tubulin sequences. This results in a new model of the tubulin monomers consisting of three major proteolytically defined regions.

Materials and Methods

Chemicals and Proteins. MES, PIPES, EGTA, SDS, BSA, PMSF, and poly(ethylene glycol) 6000 were from Sigma; Triton X-100 was from Calbiochem; paraformaldehyde and electron microscopy grade glutaraldehyde were from Merck. Monoclonal anti-α- and anti-β-tubulin antibodies (mouse ascites, DM1A and DM1B, respectively), and $Na^{125}I$ were from Amersham. Protein A (*Staphylococcus aureus*) was from Pharmacia. GTP (dilithium salt) was from Boehringer. All other chemicals were reagent grade from Merck.

Subtilisin (Carlsberg, lot 54F-0248), α-chymotrypsin (type VII, TLCK treated, lot 92F-8045), and thermolysin (lot 43F-0248) were from Sigma; trypsin (lot 1053, less than 2% chymotryptic activity) was from Calbiochem; papain (papain-dried latex) was from Koch-Light Laboratories, and protease V8 (from *S. aureus*, lots 14 and 22) was from Miles Laboratories.

Bovine brain tubulin was purified as described (Lee et al., 1973, Andreu & Timasheff, 1982). Bovine brain microtubule protein was prepared by an assembly–disassembly cycle procedure (Manso-Martinez et al., 1984). C-Terminal fragments of tubulin were prepared by digestion of 2 mg/mL purified tubulin in MMEG buffer, pH 6.6 (a total of 100 mg of tubulin), with 0.02 mg/mL subtilisin at 25 °C for 20 min. This was followed by addition of 1 mM PMSF, assembly of the cleaved protein for 30 min at 37 °C, and centrifugation at 30000*g* and 37 °C during 20 min. The supernatant, containing the small fragments, was freeze-dried, redissolved in 0.1 M ammonium bicarbonate, pH 8.5, clarified by centrifugation, separated from high molecular weight material in a (0.9 × 25 cm) Sephadex G-25 column, freed from salts and GTP in a Sephadex G-10 column equilibrated in the same buffer, and finally freeze-dried. Peptides were analyzed in a Vydac 218TP54 reverse-phase octadecyl silica column eluted with a linear gradient of acetonitrile in 10 mM HCl.

Prediction of Antigenic Determinants, Peptide Synthesis, Production of Antibodies, and Immunological Procedures. Predictions of the localization of antigenic determinants were made as described in Figure 1, by employing computer programs written in BASIC for IBM and Hewlett-Packard personal computers. Peptide synthesis, coupling to carrier proteins, and the production of rabbit antibodies are reported in detail elsewhere (Andreu et al., 1988). ELISA, indirect immunofluorescence, and immunoblotting were performed essentially as described (Andreu et al., 1988). The detection reagents for rabbit antibodies were peroxidase-labeled protein A (Amersham, diluted 1:750 in ELISA), goat anti-rabbit immunoglobulin fluoresceinated antibodies (Behring, Marburg, FRG, diluted 1:20 in immunofluorescence), and ^{125}I-labeled

[1] Abbreviations: BDB, bis-diazotized benzidine; BSA, bovine serum albumin; EGTA, [ethylenebis(oxyethylenenitrilo)]tetraacetic acid; ELISA, enzyme-linked immunosorbent assay; KLH, keyhole limpet hemocyanin; MAPS, microtubule-associated proteins; MES, 4-morpholineethanesulfonic acid; MMEG, 50 mM MES, 0.5 mM $MgCl_2$, 1 mM EGTA, and 0.1 mM GTP, pH 6.6; PBS, phosphate-buffered saline (8.1 mM disodium phosphate, 1.5 mM potassium phosphate, 137 mM sodium chloride, and 2.7 mM potassium chloride); PEM, 100 mM PIPES, 1 mM EGTA, and 1 mM $MgCl_2$, pH 6.8; PIPES, piperazine-*N*,*N*′-bis(2-ethanesulfonic acid); PMG, 10 mM sodium phosphate, 0.1 mM GTP, and 0.5 mM $MgCl_2$, pH 7.0; PMSF, phenylmethanesulfonyl fluoride; SDS, sodium dodecyl sulfate; TLCK, N^{α}-tosyllysine chloromethyl ketone.

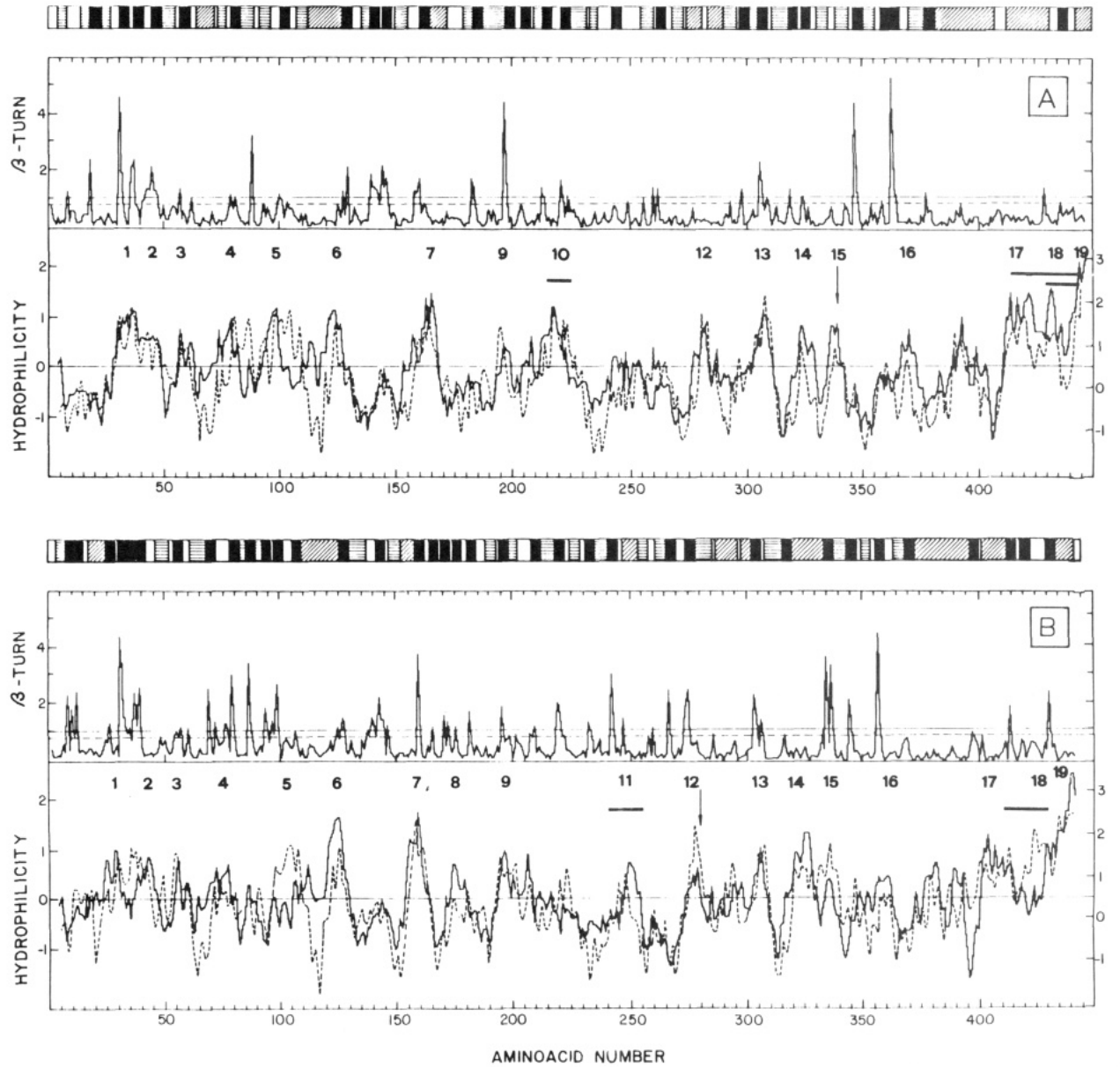

FIGURE 1: Prediction of possible antigenic determinants of α- and β-tubulin. Hydrophilicity profiles and secondary structure prediction for α-tubulin (panel A) and β-tubulin (panel B). Hydrophilicity profiles are shown in the lower part of each panel. They were made by employing the Hopp and Woods scale (continuous line, averaging hydrophobicity over seven contiguous residues along the length of the chain) and inverted Kyte and Doolittle hydrophobicity profiles (dashed line, averaging over nine contiguous residues; scale on the right ordinate); the value of the grand average of the hydropathy of 84 proteins (Kyte & Doolitle, 1982) has been made to coincide with the zero hydrophilicity value (Hopp & Woods, 1981). These two scales were selected as sufficiently different ones representative of the numerous scales proposed in the literature (Eisenberg, 1984; Rose et al., 1985), and they do give some local differences. The cleavage points by trypsin and chymotrypsin determined by Mandelkow et al. (1985a) correspond to peak α15 and β12, respectively, as indicated by the arrows. Other predictive methods such as peptide antigenicity (Welling et al., 1985) and flexibility (Karplus & Schulz, 1985) gave less clear features (not shown), most of which could be found clearly in the hydrophilicity profiles, except for a flexibility peak around position 145, corresponding to the glycine cluster which was suggested to contribute a triphosphate binding loop of the nucleotide binding site (Ponstingl et al., 1981). The upper profiles in each panel are the Chou and Fasman (1978) β-turn tetrapeptide conformation parameter. In the predictive schemes of secondary structure on top of them, the β-turn regions are marked in black, β-sheets are horizontally hatched, α-helices are obliquely hatched, and unordered structure regions are in white. The secondary structure prediction by the procedure of Garnier et al. (1978) coincided poorly in most of the sequences (not shown). The conformational preferences detected by either procedure were generally low.

protein A (approximately 2500 000 dpm/mL, sp act. 4000–17000 dpm/ng, in immunoblotting). The detection reagents for the mouse monoclonals were rabbit anti-mouse immunoglobulin peroxidase-conjugated antibodies (Dako, Glostrup, Denmark, diluted 1:400 in ELISA), sheep anti-mouse immunoglobulin fluoresceinated antibodies (Amersham, diluted 1:20 in immunofluorescence), and rabbit anti-mouse immunoglobulin antibodies ^{125}I labeled similarly to protein A (a gift of Dr. I. Barasoain from CSIC, Madrid).

Limited Proteolysis. Enzyme aliquots (1 mg/mL in 10 mM sodium phosphate, pH 7; papain was clarified by centrifugation) were stored frozen and used once. Controlled proteolysis of tubulin (2–2.3 mg/mL) was performed by incubation with protease at the indicated weight ratios (trypsin, 0.5–1%; chymotrypsin, 1–2%; subtilisin, 0.5–1%; V8 protease, 1.5–2.5%; papain, 1–1.5%; and thermolysin, 1–1.5%) in PMG buffer, pH 7.0, for 20 min, at 25 ± 0.5 °C. The reaction was stopped, the samples were electrophoresed as previously described (Andreu et al., 1986), and polypeptides were transferred electrophoretically onto nitrocellulose sheets or stained as described (Andreu et al., 1988). Apparent molecular weights of proteolytic tubulin fragments were calculated onto standard

Table I: Synthetic Tubulin Fragments and Antibody Production

peptide[a]	amino acid sequence[b]	coupling reagent and carrier employed[c]	reciprocal anti-tubulin titer[d]
α(214–226)	RRNL*DIERPTYTN	glutaraldehyde (BSA)	50 ± 20 (4)
α(430–443)	KDYEEVGV*DSVEGE	BDB (KLH)	280 ± 50 (4)
α(415–443)	EGEFSEAREDMAALEKDYEEVGV*DSVEGE	BDB (KLH)	225 ± 160 (4)
β(241–256)	RYPGQLNADLRKLAV*N	glutaraldehyde (BSA)	65 ± 25 (3)
β(412–431)	NMNDLV*SEYQQYQDATAD	glutaraldehyde (BSA)	430 ± 125 (3)

[a] α and β refer to the two tubulin in subunits. [b] The asterisk following the single-letter code indicates a tritium-labeled amino acid introduced to facilitate conjugation. All peptides were synthesized as C-terminal carboxamides. [c] Only the conjugates employed in successful immunizations are indicated. [d] Titer was arbitrarly defined as the serum dilution giving half-maximal absorption in ELISA; average, standard error, and number of animals immunized are indicated.

curves of the molecular weight markers BSA (M_r 67 000), immunoglobulin G (heavy chain, M_r 52 000; light chain, M_r 25 000), ovalbumin (M_r 43 000), and lysozyme (M_r 14 300). Reproducibility of apparent M_r values was better than 1000.

Results

Selection of Tubulin Synthetic Peptides and Specificity of the Anti-Peptide Antibodies. Hydrophilicity profiles and secondary structure predictions were calculated for the porcine brain α and β sequences (Ponstingl et al., 1981; Krauhs et al., 1981) and are shown in Figure 1. There are no strongly hydrophobic tracts in these sequences (Andreu et al., 1986), and the prediction of the secondary structure of tubulin is rather ambiguous. Nevertheless, the homologous α- and β-tubulin sequences show a number of clear hydrophilic peaks which are associated to highly probable β-turns. They are numbered in Figure 1, where we have arbitrarily counted peaks having a height larger than 1 in the scale of Hopp and Woods (1981) in any of both α and β sequences. Four small regions, each one within each of the two proteolytic domains of the α- and β-tubulin monomers considered at that time, were selected, with C- and N-terminal positions conveniently chosen to minimize predictable cross-reactivity. Since we focused on general features of the tubulin molecule, regions conserved among vertebrate tubulin isotypes (Sullivan & Cleveland, 1985) were preferred. The selected peptides are shown in Table I and marked in their corresponding positions in Figure 1. Peptides α(430–443) (epitopes α18–19), α(415–443) (epitopes α17–19), and β(412–431) (epitopes β17–18), close to the C-termini in both chains, were chosen for the involvement of these peculiarly acidic regions in the interaction with microtubule-associated proteins (see the introduction). Peptide β(241–256) (epitope β11, a hydrophilic peak within a hydrophobic valley, in which Tyr has been substituted for Phe-242) was chosen because this region may be important for colchicine binding (see the introduction). Its homologous epitope α11 is not predicted to be expressed, and a nearly corresponding region, peptide α(214–226) (epitope α10), was chosen. α(214–226) was found to be within a clear amphipathic α-helix peak in the Finer-Moore and Stroud (1984) amphipathicity algorithm, while β(241–256) showed dominant amphipathic β-sheet (2-residue period) as well as amphipathic α-helix (3.5-residue period) characteristics.

Peptides were synthesized by the solid-phase procedure (Merrifield, 1963), were purified by high-performance liquid chromatography, and had the correct amino acid composition; antibodies were reproducibly obtained from rabbits injected with the appropriate peptide–carrier conjugates, as reported elsewhere (Andreu et al., 1988).

Typical anti-tubulin titers are indicated in Table I. Controls of the specificity of these antibodies were as follows: (i) no cross-reactions among different peptides were found; (ii) the reaction of each serum with plate-adsorbed tubulin was fully displaced by soluble tubulin or the corresponding uncoupled peptide in competition ELISA; (iii) every serum reacted specifically with the α- or β-tubulin bands in immunoblots of vertebrate brain extracts; and (iv) every serum produced characteristic microtubule patterns with formaldehyde-fixed cytoskeletons of PtK2 cultured cells examined by immunofluorescence (Andreu et al., 1988). Further relevant characterization is shown by Figures 2 and 3. Figure 2A is a representative example of the reaction of the anti-β(241–256) serum with glutaraldehyde-fixed microtubules of PtK2 cytoskeletons. The specificity of this immunofluorescence was verified by treatment of the cells with a bicyclic colchicine analogue (Diez et al., 1987), resulting in depolymerization of the microtubule network (Figure 2B), and by preincubation of the sera with tubulin or the corresponding peptides, resulting in lack of reaction with the cytoskeletons (Figure 2C). Panels D and E,F of Figure 2 show the staining of the marginal band of chicken erythrocytes and plant microtubules, respectively, by the anti-β(412–431) serum. Figure 3 shows the cross-reactions found in the case of the overlapping peptides α(415–443) and α(430–443), which show that the antiserum to the larger peptide recognizes determinants in the α(430–443) region homologous to the short peptide as well as in the α-(415–429) region not embraced by this peptide.

Synthetic Peptide Mapping of Determinants Recognized by the Anti-Tubulin Monoclonal Antibodies DM1A and DM1B. The reactivity of the synthetic peptides with the DM1A and DM1B monoclonal antibodies (Blose et al., 1984) was examined and compared to that of tubulin. In direct ELISA with carrier-coupled peptides, DM1A reacted with α(415–443) but not with peptides α(430–443) or β(412–431), while DM1B did not react significantly with any of the peptides (not shown). Figure 4A is a competitive ELISA with the uncoupled peptides, showing that the reaction of DM1A with tubulin is fully displaced by α(415–443) and not affected by either α(430–443) or β(412–431). The latter peptide displaces the reaction of DM1B with tubulin, which is in turn unaffected by the α peptides. These results clearly indicate that the segment α(415–430) contains residues recognized by DM1A and that peptide β(412–431) is recognized by DM1B in its uncoupled form, but not when it has been chemically modified by either glutaraldehyde or BDB. When the competition by the free peptides (Figure 4A) was compared with the competition by tubulin in stabilizing buffer (Figure 4B), it became apparent that tubulin concentrations roughly similar to those of α(415–433) displaced the reaction, whereas tubulin concentrations 20 times smaller than those of β(412–431) were about equally effective as the peptide.

To support the observations of Figure 4A with a different technique and materials, we performed indirect immunofluorescence experiments with the DM1A and DM1B monoclonals and the peptides on cytoskeletons of PtK2 cells. The results, summarized by Figure 5, show that cellular microtu-

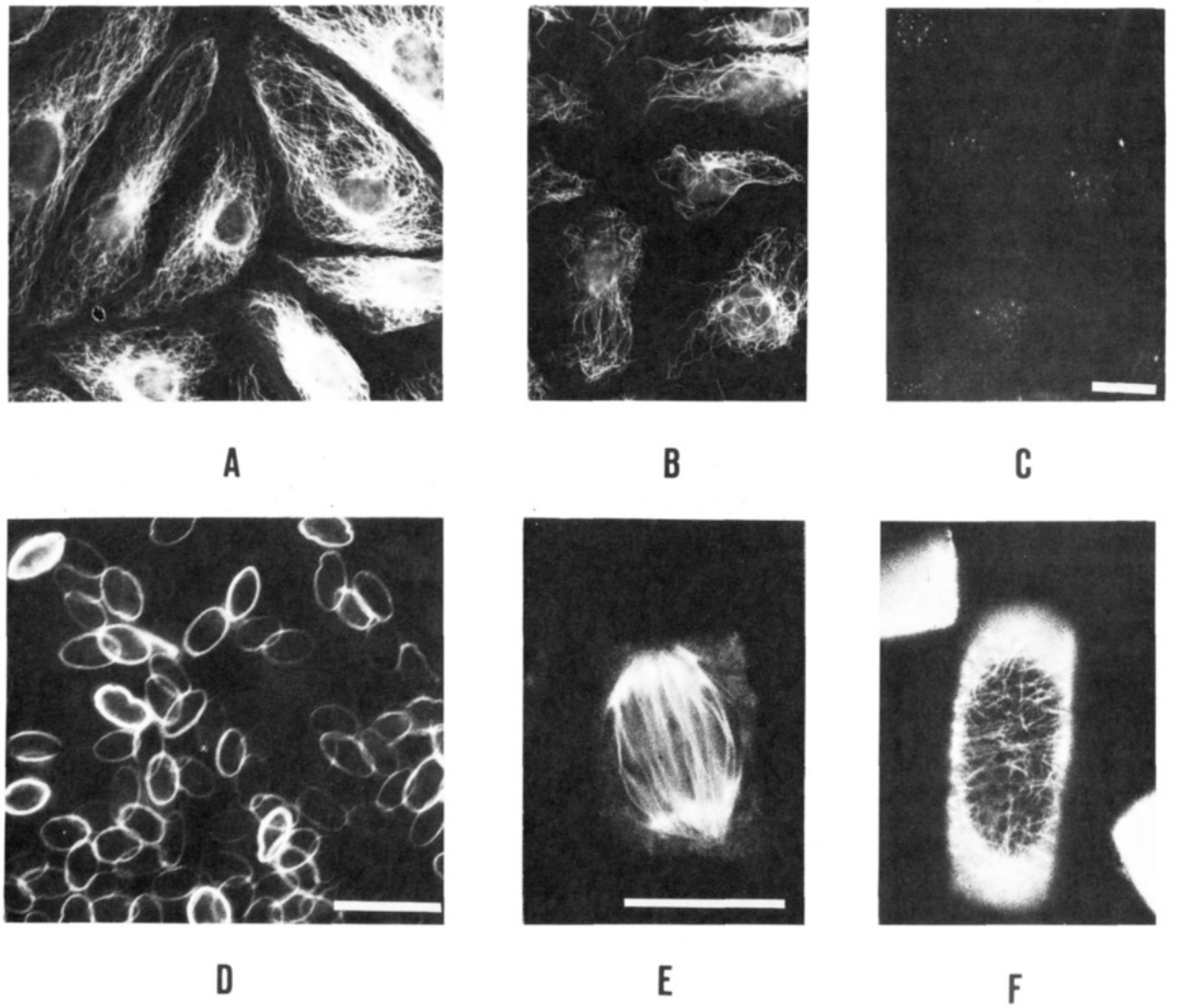

FIGURE 2: Microtubules from different systems visualized by anti-peptide antisera in indirect immunofluorescence. Panel A: Cytoskeletons from PtK2 cultured cells were fixed with 0.5% glutaraldehyde in PEM for 15 min at room temperature, followed by 2 mg/mL sodium borohydryde in PBS, and processed with anti-β(241–256) serum (1:30 dilution). The antiserum had been pretreated with glutaraldehyde-cross-linked BSA in order to reduce nonspecific background caused by antibodies to glutaraldehyde-modified protein. Panel B: Same, with cells treated with the bicyclic colchicine analogue (2 μM). Panel C: A negative control of the anti-peptide antisera adsorbed with purified tubulin (0.1 mM). Same results as in panel C were obtained by adsorption of the antibodies with peptide β(241–256). Equally negative results were obtained with nonimmune sera or sera to the nonrelated peptide Met-enkephalin. Panel D: Reaction of anti-β(412–431) serum (1:50 dilution) with the marginal band of chicken erythrocyte cytoskeletons fixed with formaldehyde. Chicken erythrocytes were prepared by mixing fresh blood with 1 volume of Alserver's solution (Chanock & Sabin, 1953), centrifuged (400*g* for 10 min at room temperature), washed twice with 0.9% NaCl, let to adsorb for 10 min onto glass cover slips, and processed for immunofluorescence. Panels E and F show the reaction of the same antiserum with microtubules from *Allium* root cells. Root tip cells were prepared for indirect immunofluorescence localization of microtubules according to the method of Wick et al. (1981) with modifications (Clayton & Lloyd, 1984). Bars indicate 20 μm.

bules visualized with DM1A and DM1B do not react significantly when these antibodies have been adsorbed with α-(415–443) and β(412–431), respectively.

Mapping of Tubulin Proteolytic Fragments by Anti-Peptide Antibodies. We have systematically employed the anti-peptide antibodies to identify fragments of limited cleavage of tubulin by trypsin, chymotrypsin, papain, thermolysin, V8 protease, and subtilisin. The identification and alignment of the segments on the tubulin sequence reported here is based exclusively on their reactivity with the antibodies and is therefore meant to be unequivocal, except where noted. However, the size and exact limits of the fragments are estimated from their electrophoretic mobility and constitute only approximations.

Trypic and Chymotryptic Fragments. Figure 6A shows representative results of the limited proteolysis of tubulin with trypsin (predominantly α-tubulin) or chymotrypsin (predominantly β-tubulin). The positioning of the tryptic and chymotryptic fragments into the tubulin sequence is shown by Figure 6B and Table II, as well as their apparent size. The main tryptic fragments together approximately make the apparent length of the α chain. This chain behaves anomalously in the electrophoretic system, giving an apparent M_r 6000 in excess of its sequence molecular weight. However, in the case of β-tubulin, whose apparent and real molecular weights are closer, the result of adding the main chymotryptic fragments apparently exceeds the length of the chain. This clearly points out the inadequacy of apparent (electrophoretic) molecular weights to accurately measure the size of the fragments.

Papain and Thermolysin Fragments. These two proteases degraded both α and β chains and gave more complex cleavage patterns, shown in Figure 7A and analyzed in Figure 7B and Table II. Besides the internal cleavages shown, the lack of reaction of any band of papain-treated tubulin with anti-α-(430–443) suggests a cleavage point a few amino acids from the C-terminus. The bands Pa4 and Th6, which do not react with any of the antibodies, could correspond to N-terminal

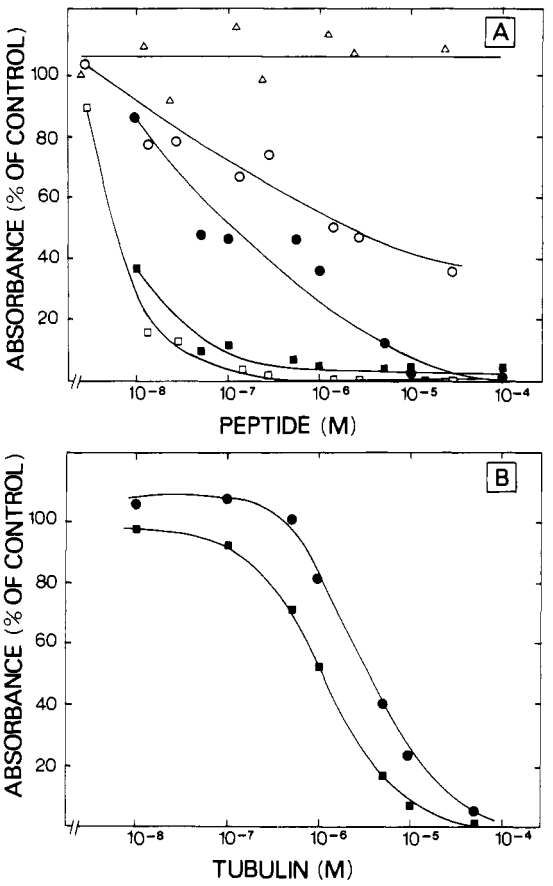

FIGURE 3: Cross-reaction of rabbit anti-peptide antisera examined by competition ELISA. Plates were coated with tubulin. Panel A: Reaction of antibodies with soluble peptides. Solid circles, anti-α-(415–443) (1:100 dilution) preincubated with the indicated concentrations of peptide α(415–443); open circles, same serum preincubated with the shorter peptide α(430–443); solid squares, anti-α(430–443) (1:100 dilution) preincubated with α(415–443); open squares, same serum preincubated with α(415–430); open triangles, anti-α(430–443) preincubated with peptide β(412–431). Results are expressed as percent of controls of antisera preincubated without competing peptides. Panel B: Reaction of anti-peptide antibodies with soluble tubulin. Circles, anti-α(415–443); squares, anti-α(430–443).

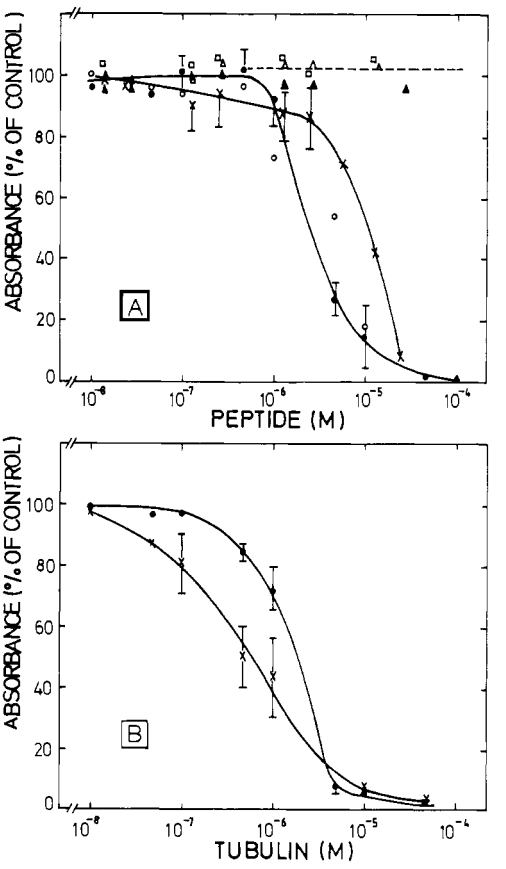

FIGURE 4: Competition ELISA of the DM1A and DM1B anti-tubulin monoclonal antibodies. DM1A (1:12600 dilution) and DM1B (1:1600 dilution) ascitic fluids were preincubated with the indicated concentrations of peptides (panel A) or purified tubulin (panel B). Panel A: Reaction of DM1A with α(415–443) is represented by solid circles; [DM1A with α(415–443) under tubulin-stabilizing conditions (open circles) gave comparable results]; with α(430–443), by open triangles; and with β(412–431), by open squares. Preincubation of DM1B with α(430–443) is indicated by solid triangles; with β(412–431), by crosses. The average of two different assays is shown. Panel B: Preincubation of DM1A and DM1B (solid circles and crosses, respectively) with soluble tubulin under stabilizing conditions. The average of two different assays is represented. Curves are drawn solely to show the trend of the data.

peptides generated by the same cleavage as the peptides detected in the immunoblots.

Subtilisin and Protease V8 Fragments. Figure 8A shows the results of limited digestion of tubulin by subtilisin in PMG buffer and in MMEG buffer. Terminal (Sbα, Sbβ) and internal Sb3 to Sb6) chain cleavage products are observed in both buffers; the internal cleavage is more extensive in the first buffer. The results are analyzed in Figure 8C and Table II. Sbα is not recognized by anti-β antibodies, and anti-α antibodies do not react with Sbβ. Sbα is recognized by anti-α-(430–443) less intensely than the intact chain (at high subtilisin/tubulin ratios this reaction practically disappears). However, Sbα reacts with anti-α(415–443) more intensely than the intact chain, and the band in the blot smears into the higher mobility region of β (see Figure 8A and also Figure 9A, lane 8). Sbα reacts with anti-α(214–226) with a similar smear and an intensity comparable to that of the intact α chain. Therefore, Sbα is heterogeneous and results from a minimum of two C-terminal cleavages, one (Sbα1) slightly damaging the antigenic reactivity of the α(430–443) region (that is, about position 440) and another cleavage (Sbα2) that essentially removes this region while enhancing the reactivity to the anti-α(415–443) antiserum. Since this serum contains antibodies that recognize determinants in both the α(415–430) and α(430–443) regions (Figure 3), Sbα2 results from cleavage at about position 430. These results are fully consistent with the fact that Sbα reacted like the intact α chain with the monoclonal antibody DM1A (not shown), which recognizes determinants in the α(415–430) region as shown above (Figures 4 and 5). That subtilisin cleavage of α-tubulin generating Sbα is C-terminal and not N-terminal was further verified by double digestion experiments with trypsin and subtilisin, shown by Figure 8B, lanes 1–7. Similarly, Sbβ consists of the product(s) of C-terminal cleavage of the β chain as shown by double digestion experiments with chymotrypsin and subtilisin (Figure 8B, lanes 8–13). Sbβ reacts with anti-β(412–431) comparably to the intact chain, indicating cleavage point(s) approximately between position 430 and the C-terminus. This result is consistent with the fact that Sbβ reacted with the monoclonal antibody DM1B (not shown), which recognizes determinants in the β(412–431) region (Figures 4 and 5). However, the decrease in apparent molecular weight would erroneously suggest the cleavage of most of this antigenic region. This is again an example of how dodecyl sulfate electrophoresis is not an adequate procedure to accurately determine the size of the tubulin fragments.

The results with microtubule protein indicated subtilisin digestion patterns and antibody reactivities qualitatively similar to purified tubulin (Figure 8B, lanes 14–21). In an attempt

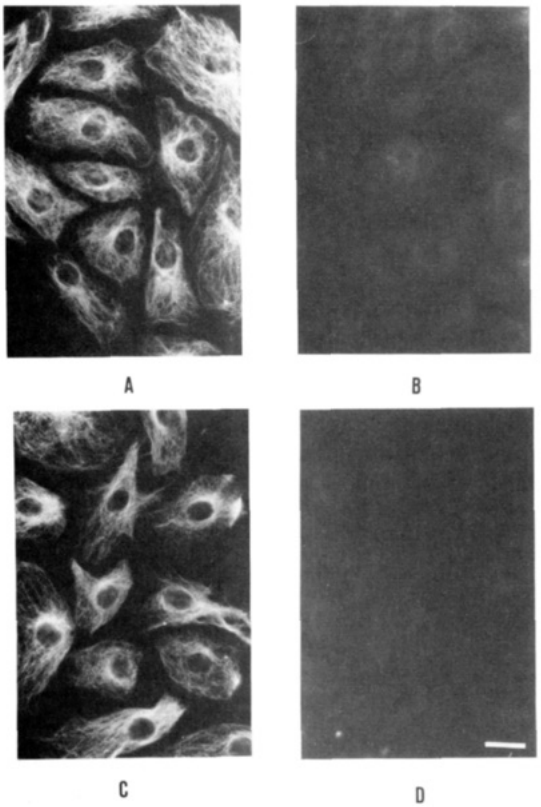

FIGURE 5: Indirect immunofluorescence competition assay of DM1A and DMB1B monoclonal antibodies on formaldehyde-fixed PtK2 cytoskeletons. Panel A: DM1A adsorbed with free β(412–431). Panel B: DM1A adsorbed with α(415–443). Panel C: DM1B adsorbed with α(430–443). Panel D: DM1B adsorbed with β(412–431). DM1A adsorbed with α(430–443) and DM1B adsorbed with α-(415–443) gave results similar to panels A and C (not shown). All pictures are exposed for the same time, except panel B, in which the negative was deliberately overexposed 5 times in order to show the weak fluorescence observed. The bar indicates 20 μm.

to determine more accurately the C-terminal subtilisin cleavage points on α- and β-tubulin, we prepared the small C-terminal fragments from a batch digestion of tubulin and subjected them to reverse-phase high-performance liquid chromatography (Materials and Methods). Approximately 30 peaks eluted in the 2–50% region of the acetonitrile gradient. This suggested a marked heterogeneity of the subtilisin cleavage products (possibly sequential cleavage), and a further characterization of the individual peptides was not performed.

Similarly to subtilisin, the protease V8 from *S. aureus* produces terminal and internal cleavages of tubulin (Figure 9 and Table II). Terminal cleavage is preferential on β-tubulin and gives a minimum of two apparently sequential products, V81 and V82. These are most probably the result of C-terminal cleavage and not of N-terminal cleavage, since double digestion with V8 protease and subtilisin (Figure 9, lanes 3, 15, and 23) gave essentially the C-terminal subtilisin cleavage product Sbβ and not the two hypothetical higher mobility species that would result from its further N-terminal cleavage; double digestion with V8 and chymotrypsin afforded confirmatory results (not shown). V81 reacts with anti-β(241–256) and anti-β(412–431) antibodies, indicating that the corresponding cleavage point is located approximately between positions 430 and the C-terminus, although the decrease in apparent molecular weight could suggest a more internal cleavage. V82 reacts with anti-β(241–256) and weakly and less reproducibly with anti-β(412–431), indicating cleavage at the β(412–431) region. We occasionally observed a further digestion product, V82′ at higher V8 to tubulin ratios. The internal cleavage products predominantly derive from α-tubulin.

Table II: Analysis of Tubulin Proteolytic Fragments[a]

protein band		components		
name	app M_r[b]	app no. of residues[c]	chain	sequence position
Tr1	37 600 ± 1000	321 ± 27	α	contains α(214–226)
Tr1′	35 000 ± 2000	299 ± 34	α	contains α(214–226)[d]
Tr2	17 200 ± 900	147 ± 17	α	321 ± 27 to 450
Ch1	34 300 ± 1300	303 ± 14	β	contains β(241–256)
Ch1	34 300 ± 1300	293 ± 28	α	157 ± 28 to 450[d,e]
Ch1′	30 200 ± 400	267 ± 20	β	contains β(241–256)[d]
Ch2	20 800 ± 1200	184 ± 12	β	282 ± 24 to 445
Pa1	34 700 ± 700	296 ± 23	α	139 ± 23 to ~435
Pa1	34 700 ± 700	306 ± 9	β	139 ± 9 to 445[f]
Pa1′	32 700 ± 800	288 ± 9	β	157 ± 9 to 445[d]
Pa2	20 000 ± 800	171 ± 16	α	264 ± 16 to ~435[g]
Pa2	20 000 ± 800	171 ± 16	α	contains α(214–226)[g]
Pa2	20 000 ± 800	176 ± 8	β	269 ± 8 to 445[d]
Pa2	20 000 ± 800	176 ± 8	β	contains β(241–256)[d]
Pa3	17 800 ± 800	152 ± 16	α	283 ± 16 to ~435[g]
Pa3	17 800 ± 800	152 ± 16	α	contains α(214–226)[g]
Pa4	16 800 ± 400	142 ± 9		*h*
Th1	38 200 ± 1000	325 ± 28	α	125 ± 28 to 450[d]
Th2	34 000 ± 800	289 ± 23	α	161 ± 23 to 450[f]
Th2	34 000 ± 800	299 ± 10	β	146 ± 10 to 445[f]
Th3	32 000 ± 600	273 ± 20	α	177 ± 20 to 450[d,f]
Th3	32 000 ± 600	283 ± 8	β	162 ± 8 to 445
Th3	32 000 ± 600	283 ± 8	β	contains β(241–256)[d]
Th4	20 400 ± 1000	173 ± 18	α	277 ± 18 to 450[d,e]
Th5	19 000 ± 800	162 ± 15	α	288 ± 15 to 450[g]
Th5	19 000 ± 800	162 ± 15	α	contains α(214–226)[g]
Th6	17 700 ± 1000	151 ± 16		*h*
Sbα1	54 700 ± 1100	440 ± 9	α	1 to ~440
Sbα2	51 500 ± 1200	415 ± 9	α	1 to ~430
Sbβ	48 000 ± 900	419 ± 8	β	1 to ~431
Sb3	36 200 ± 700	309 ± 23	α	contains α(314–226)
Sb4	34 000 ± 1400	289 ± 28	α	141 ± 28 to ~430
Sb4	34 000 ± 1400	297 ± 15	β	contains β(241–256)
Sb5	19 200 ± 1100	164 ± 19	α	266 ± 19 to ~430
Sb6	18 200 ± 800	156 ± 15	α	274 ± 15 to ~430
V8 1	46 200 ± 400	416 ± 8	β	1 to ~430
V8 2	44 800 ± 900	403 ± 8	β	1 to ~420
V8 3	34 800 ± 700	296 ± 23	α	154 ± 26 to 450
V8 4	27 100 ± 500	230 ± 19	α	220 ± 19 to 450[d,e]

[a] The different peptides were identified and aligned on the basis of the antigenic reactivities shown by Figures 6–9. [b] Molecular weights determined by SDS–polyacrylamide gel electrophoresis. [c] The errors given include the differences that result from employing the real [50 000, 450 residues, Ponstingl et al. (1981); 49500, 445 residues, Krahus et al. (1981)] or the apparent molecular weights (56 000 ± 800; 50 900 ± 700) of α- and β-tubulin in the calculations. [d] Minor component. [e] Probable species. [f] Species not confirmed by its failure to react with anti-α(214–226) or anti-β(241–256). [g] The apparent size of this band is considerably smaller than the minimal size of a single peptide containing the antigenic signals detected; it consists of the two components indicated in the table. [h] Not detected by our antibodies.

The approximate location of the minimum number of terminal cleavage points by V8 and subtilisin are indicated in Figure 10, where the parts of the tubulin sequence embraced by the synthetic peptides are underlined by a continuous tracing.

Figure 11 summarizes the approximate cleavage points of the α- and β-tubulin chains by the six proteases. Peptides of clear existence yet of imprecise location such as Tr1′, Ch1′, Pa2, Pa3, Th3 (β), Sb3, and Sb4 (β) (Table II) are not considered. For this reason, for other possibly undetected products and the limited number of proteases employed, this is a minimal proteolytic map of tubulin, which does not exclude other cleavage sites. The cleavage points determined cluster in three regions (shaded in Figure 11) approximately corre-

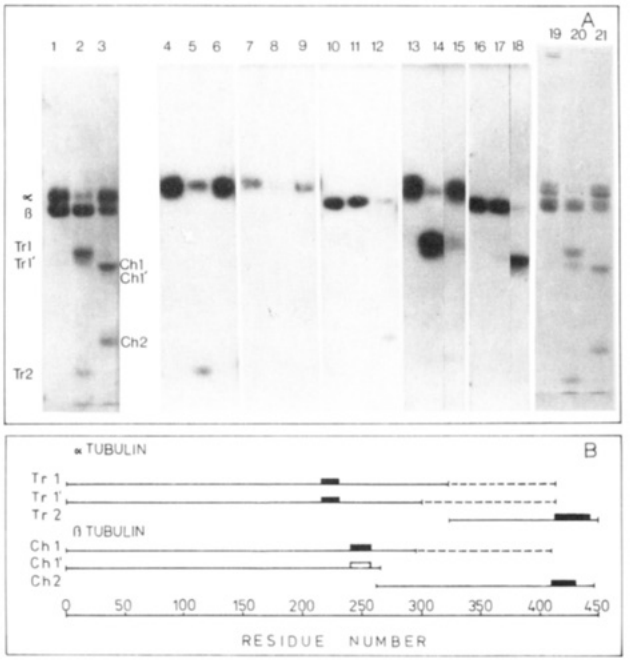

FIGURE 6: Limited proteolysis of brain tubulin by trypsin and chymotrypsin. SDS gel electrophoresis was made in a 10% acrylamide gel. Panel A: Lanes 1, 4, 7, 10, 13, and 16, purified bovine brain tubulin; lanes 2, 5, 8, 11, 14, and 17, trypsin-digested tubulin (1% w/w); lanes 3, 6, 9, 12, 15, and 18, chymotrypsin-digested tubulin (2% w/w). Lanes 1–3 are a gel section stained with Coomassie blue, and the rest of the lanes are autoradiographies of blots processed with different antipeptide antisera: lanes 4–6 with anti-α(415–443) (1:100 dilution), lanes 7–9 with anti-α(430–443) (1:30 dilution), lanes 10–12 with anti-β(412–431) (1:50 dilution), lanes 13–15 with anti-α(214–226) (1:25 dilution), and lanes 16–18 with anti-α(241–256) (1:25 dilution). Limited proteolysis of calf brain microtubular protein by trypsin and chymotrypsin is shown by the Coomassie-stained lanes 19 (microtubular protein), 20 (digested by trypsin), and 21 (digested by chymotrypsin) (SDS gel electrophoresis was made in a 9% acrylamide gel); antibody reactivity of the fragments was the same as for purified tubulin (not shown). Panel B: Alignment of the tryptic and chymotryptic fragments into the tubulin sequence. The antigenic signals observed for each peptide in the original blots are indicated by solid rectangles (strong signals) or open rectangles (weak signals, sometimes difficult to appreciate in the photographs) in their corresponding sequence positions. Dashed lines indicate the limits to the position of the fragments.

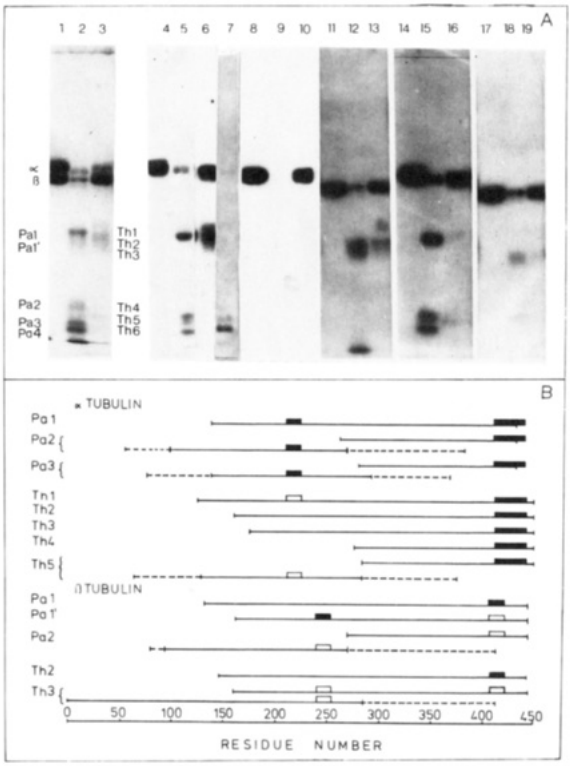

FIGURE 7: Limited proteolysis of tubulin by papain and thermolysin. SDS gel electrophoresis was carried out in a 9% acrylamide gel. Panel A: Lanes 1, 4, 8, 11, 14, and 17, purified tubulin; lanes 2, 5, 9, 12, 15, and 18, papain-digested tubulin (1.5% w/w); lanes 3, 6, 10, 13, 16, and 19, thermolysin-digested tubulin (1.5% w/w); lane 7, tubulin digested by thermolysin in a different experiment which shows the antigenic reactivity of the small molecular weight fragments. Lanes 1–3 are stained with Coomassie blue, and lanes 4–7 were processed with anti-α(415–443), lanes 8–10 with anti-α(430–443), lanes 11–13 with anti-β(412–431), lanes 14–16 with anti-α(214–226), and lanes 17–19 with anti-β(241–256). Panel B: Scheme of tubulin fragments produced by limited proteolysis by papain and thermolysin.

sponding to residues 115–165, 260–300, and the C-terminus in both chains.

Discussion

Properties of Antibodies to Tubulin Synthetic Peptides. Two strategies frequently employed to obtain antibodies against small determined regions of a protein are monoclonal antibodies to the protein followed by the mapping of their epitopes or the immunization with peptides from the protein sequence. In the latter case the selection of appropriate peptides is a crucial step. Antigenicity prediction for proteins of unknown three-dimensional structure has been the subject of a number of approaches, such as segmental hydrophilicity or accessibility (Hopp & Woods, 1981; Rose et al., 1985), predicted segmental mobility (Karplus & Schultz, 1985), and antigenic peptide detection (Welling et al., 1985) among others. In our case a combination of simple hydrophilicity and secondary structure (β-turn) algorithms (Figure 1) was employed to choose five tubulin peptide sequences, all of which successfully elicited antibodies cross-reactive with this weakly immunogenic protein, when they were employed in the appropriate carrier-coupled forms [Table I and Andreu et al. (1988)]. The fact that the antibodies react with soluble as well as plate-adsorbed tubulin is a qualitative indication that their determinants are exposed in the tubulin heterodimer, which remains open to further experimental testing under rigorous tubulin stability conditions. The antibodies react specifically with the regions of the protein spanned by the peptides and recognize specifically fixed cellular microtubules from several sources [Figures 2 and 3 and Andreu et al. (1988)]. Actually, peptides selected were of zones as conserved as possible among the known tubulin isotype sequences in different organisms, and therefore these antibodies are expected to have a very wide reactivity. The reaction of anti-β(412–431) with the marginal band of chick erythrocytes suggests that a homologous region is conserved in erythrocyte β-tubulin even though this protein shows altered electrophoretic mobility and properties which may indicate C-terminal modifications (Murphy & Wallis, 1983). The titers of the tubulin anti-peptide antibodies were not high (Table I). This possibly reflects a widespread limitation of simple linear peptides to mimic more complex protein epitopes, as illustrated by the crystallographic structure of a lysozyme–monoclonal antibody complex (Amit et al., 1986). From the results of the present study it might be expected that most tubulin anti-peptide antibodies will be useful as antigenic site probes although their use as high-affinity perturbants (such as to inhibit assembly) may be restricted to favorable cases. For these purposes large quantities of high-affinity tubulin-cross-reactive monoclonal antibodies might be obtained by immunization with the peptides and appropriate hybridoma selection. We presently attempt to measure the binding of the anti-peptide antibodies

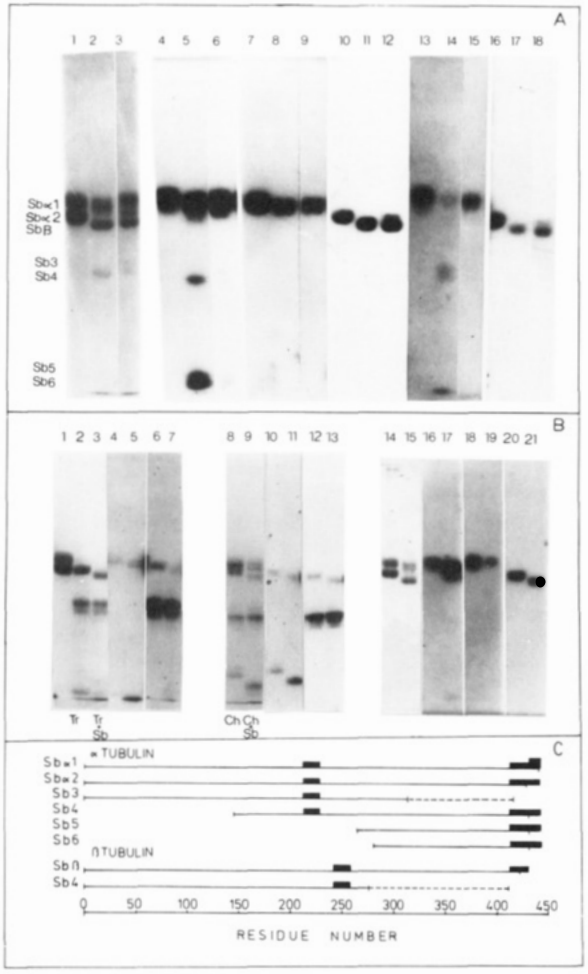

FIGURE 8: Limited proteolysis of tubulin with subtilisin. SDS electrophoresis was made in a 9% acrylamide gel. Panel A: Lanes 1, 4, 7, 10, 13, and 16, purified bovine brain tubulin; lanes 2, 5, 8, 11, 14, and 17, tubulin digested in PMG buffer, pH 7.0 (1% subtilisin/tubulin); lanes 3, 6, 9, 12, 15, and 18, tubulin digested in MMEG buffer, pH 6.6 (1% subtilisin/tubulin). Lanes 1–3 were stained with Coomassie blue, and lanes 4–6 were processed with anti-α(415–443), lanes 7–9 with anti-α(430-443), lanes 10–12 with anti-β(412–431), lanes 13–15 with anti-α(214–226), and lanes 16–18 with anti-β-(241–256). Panel B: Lanes 1–7 show a double digestion experiment with trypsin and subtilisin. Lanes 2, 4, and 6, digestion by trypsin (0.85% w/w); lanes 3, 5, and 7, digestion by trypsin (0.85% w/w) and subtilisin (0.43% w/w). Lanes 1–3 were stained with Coomassie blue, and lanes 4 and 5 were processed with anti-α(415–443) and lanes 6 and 7 with anti-α(214–226). Lanes 8, 10, and 12, digestion by chymotrypsin (1.8% w/w); lanes 9, 11, and 13, double digestion by chymotrypsin (1.8% w/w) and subtilisin (0.43% w/w). Lanes 8 and 9 were stained with Coomassie blue, and lanes 10 and 11 were processed with anti-β(412–431) and lanes 12 and 13 with anti-β(241–256). Lanes 14–21, subtilisin digestion of calf brain microtubular protein. Lanes 14, 16, 18, and 20, nondigested microtubule protein; lanes 15, 17, 19, and 21, microtubule protein digested by subtilisin (1.4% w/w). Lanes 14/15, 16/17, 18/19, and 20/21 were stained with Coomassie and processed with anti-α(415–443), anti-α(430–443), and anti-β-(412–431), respectively. Panel C: Scheme of tubulin fragments produced by limited proteolysis with subtilisin.

to native tubulin and native microtubules.

Among the few monoclonal antibodies to tubulin that are widely available, YL 1/2 (Kilmartin et al., 1982) was the only antibody whose protein determinant had been localized at the tyrosinated C-terminus of the α chain (Wehland et al., 1983, 1984). Coincidence of the epitopes defined by the YOL 1/34 (Kilmartin et al., 1982) or the DM1A and DM1B monoclonal antibodies (Blose et al., 1984) with any of the regions homologous to the peptides synthesized by us was initially considered not a very predictable event. However, cross-reactions

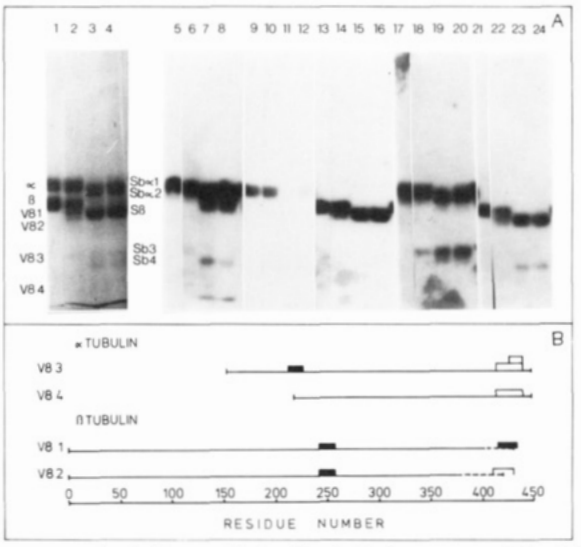

FIGURE 9: Limited proteolysis of tubulin by protease V8. SDS electrophoresis was made in a 7.5% acrylamide gel. The first lane of each group is tubulin, the second is tubulin digested with V8 protease (1.5% w/w), the third is a double digestion of tubulin with V8 (1.5% w/w) and subtilisin (0.5% w/w), and the fourth column is tubulin digested with subtilisin (0.5% w/w). Lanes 1–4 were stained with Coomassie blue and the other groups processed with the antibodies, in the same order as Figure 8A.

were found. In a study with a number of peptides derived from extensive proteolytic and chemical cleavage of tubulin, Breitling and Little (1986) have reported that determinants recognized by YOL 1/34, DM1A, and DM1B map in positions α(414–422), α(426–430), and β(416–430) respectively. The two latter positions are embraced by our synthetic peptides α(415–443) and β(412–431), respectively. In contrast to this, an alternative view based on previously estimated cleavage points by trypsin chymotrypsin, and particularly subtilisin has indicated that DM1A recognizes determinants in the α(339–390) region and DM1B in the β(339–407) region (Serrano et al., 1986b), which are more internal to the tubulin chains and not embraced by the synthetic peptides. We have found that the synthetic positions α(415–430) effectively displace the reaction of DM1A with tubulin-coated ELISA plates or fixed cellular microtubules (Figures 4 and 5). Reactivity of α(415–443) with DM1A is comparable to that of tubulin. The peptide β(412–431) similarly binds in solution to DM1B, although in this case the synthetic peptide is much less reactive than tubulin. The implication seems to be that DM1B recognizes as well other residues or conformations not contained in the peptides. This provides an independent confirmation based on chemical synthesis of the location of the DM1A and DM1B antigenic regions by Breitling and Little (1986) (see Figure 11). Preliminary results indicate that the reaction of YOL 1/34 with tubulin is displaced by the peptide α(415–443) (S. de la Viña and J. M. Andreu, unpublished results). The fact that the monoclonal antibodies mapped so far are directed against both α and β C-termini suggests that these are major immunogenic regions of this protein.

Identification of Fragments of Limited Proteolysis of Tubulin by Anti-Peptide Antibodies. Application of limited proteolysis to structural and functional studies of tubulin has been a controversial subject (see the introduction). One the other hand, the noncovalent structure of purified soluble tubulin has a limited stability; the protein partially unfolds, loses activity, and aggregates readily under standard conditions (Andreu & Timasheff, 1982; Prakash & Timasheff, 1982). We have employed very mild conditions [see Materials and

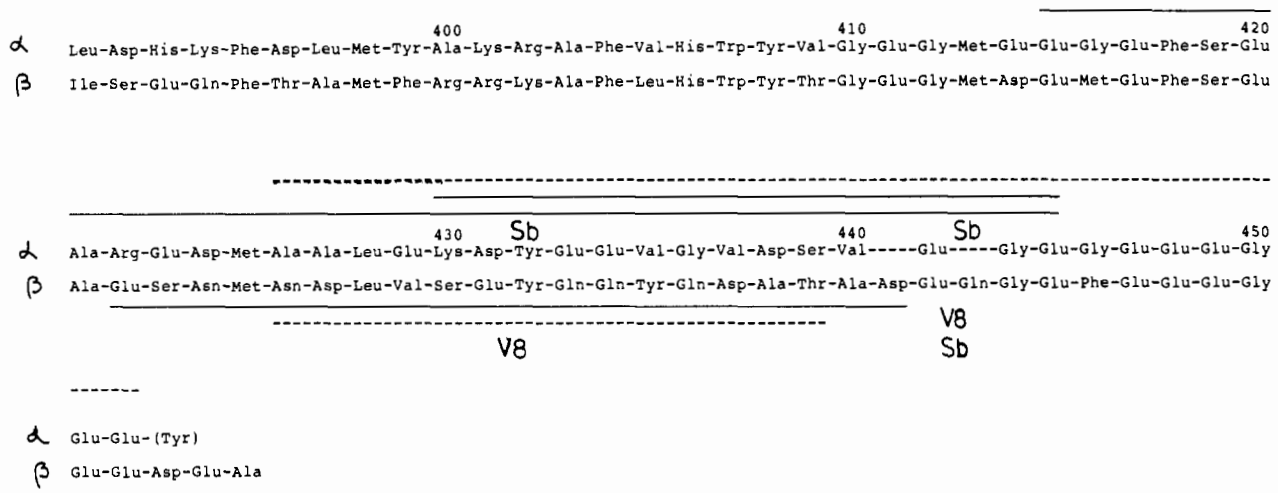

FIGURE 10: Carboxy-terminal sequences of porcine brain α- and β-tubulin [after Postingl et al. (1981) and Krauhs et al. (1981)]. The synthetic peptides corresponding to these regions are indicated by solid lines. The long α peptide binds to the DM1A monoclonal antibody, while the shorter peptide does not; the β peptide binds to the DM1B monoclonal antibody (Figures 4 and 5 and Results). The regions determined by Breitling and Little (1986) to be recognized by DM1A and DM1B, employing peptides from extensive proteolytic and chemical degradation of porcine tubulin, are indicated by the dashed lines. The approximate cleavage points by V8 and subtilisin are shown solely to indicate the cases in which these proteases do or do not remove the antigenic zones defined by the synthetic peptides (Figures 8 and 9 and Results).

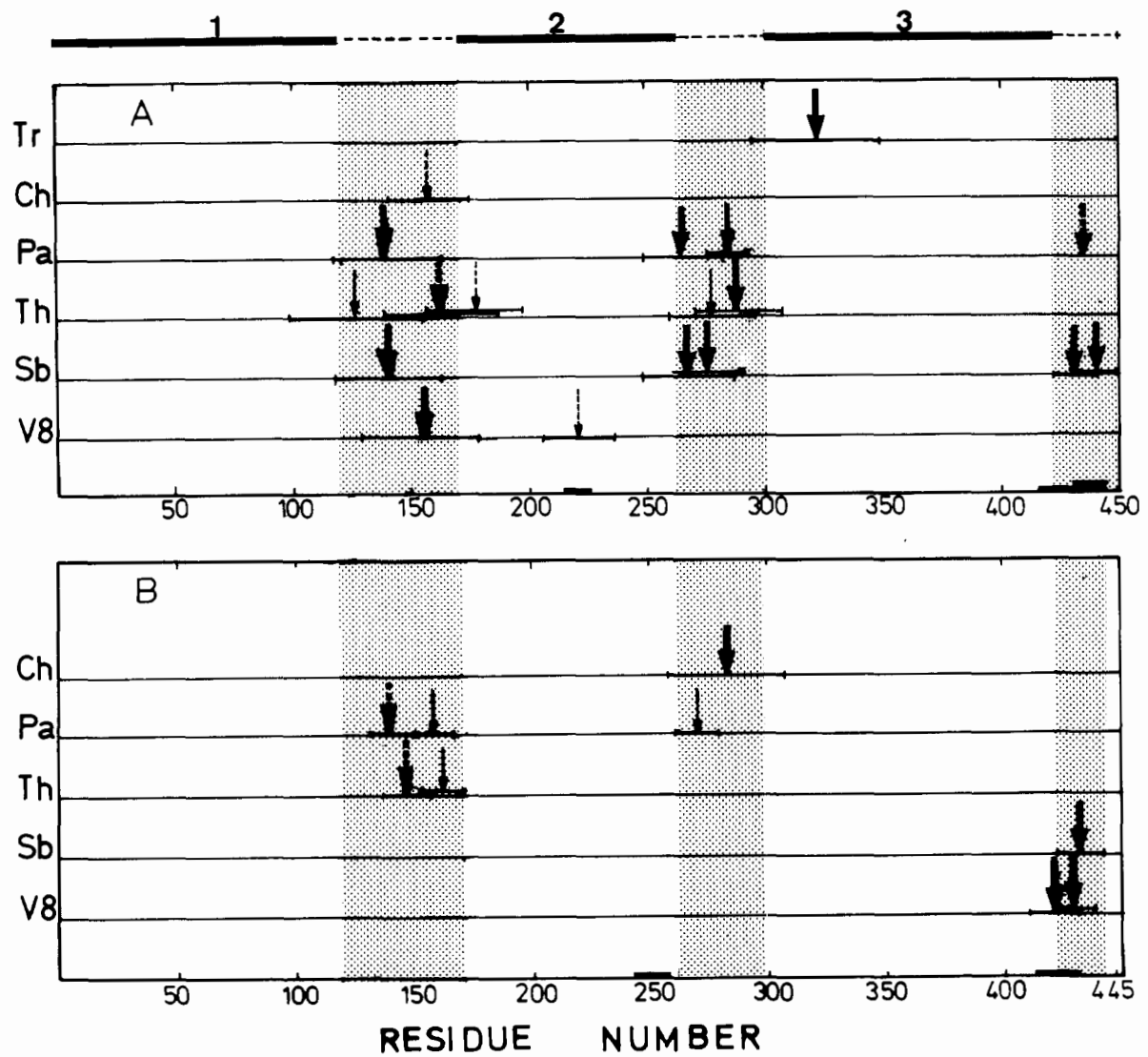

FIGURE 11: Map of the limited cleavage of native tubulin by six proteases. This map summarizes the approximate cleavage points for each protease on α- (panel A) or β-tubulin (panel B). Solid arrows indicate the confirmed cleavages, and dashed arrows indicate probable cleavages which were not fully confirmed (see the text). Arrows in heavy tracing represent predominant cleavages, and fine tracing indicates minor cleavages. The alignment of the fragments is the same as in the schemes of Figures 6–9, while the large error bars shown are the results of the imprecision of molecular weight estimations by gel electrophoresis (Table II).

Methods and Andreu et al. (1986)] under which the limited cleavage of the native protein should be favored over the more extensive cleavage pattern of partially unfolded forms. The use of anti-peptide antibodies has provided a self-consistent procedure enabling us to unequivocally align well-reproducible peptide fragments into the tubulin sequences (Results). The only assumption in this procedure is that the antibodies are fully specific for the protein regions homologous to the synthetic peptides. This has been supported by all our tests [Figure 3 and Andreu et al. (1988)] and the fact that the antibodies to one chain did not cross-react with the other chain (Figures 6–9). The reaction with other (sequence-unrelated) regions within the same chain is improbable and would be expected to systematically give nonconsistent mapping results.

Our tryptic and chymotryptic cleavage patterns are confirmatory, by employing a different tubulin source and experimental approach, to the main cleavages reported by Mandelkow et al. (1985a). We find that the present evidence is not compatible with the report by Maccioni and Seeds (1983) indicating chymotryptic cleavage of both α- and β-tubulin at Phe-135 and Phe-133, respectively. However, proteolytic cleavages at roughly one-third from the N-termini in both chains do take place with other proteases. A number of proteolytic enzymes were known to cleave the tubulin chains into characteristic large fragments of about two-thirds of the chain length and small fragments comprising roughly one-third of the chain (Kirchner & Mandelkow, 1985; J. M. Andreu, unpublished results). By comparison to the trypsin and chymotrypsin patterns, one may tend to assume that the cleavage points by the other proteases are in the same region, roughly located at two-thirds of the chain length from the N-termini. Sackett & Wolff (1986) have reported that clostripain, Pronase, and papain generate proteolysis patterns on rat brain tubulin that are very similar to those of trypsin and chymotrypsin. They have proposed a large domain–small domain model of tubulin which assumes that all their proteases cleave the same region connecting the two domains. In contrast, the identification of the fragments of limited proteolysis with anti-peptide antibodies clearly indicates that in our experimental system papain cleaves α- and β-tubulin at both approximately one-third and two-thirds of the chain length (Figure 8). Furthermore, other proteases, such as thermolysin, subtilisin, and V8, also cleave at one-third of the chain length (see Figure 11).

Subtilisin, V8, and possibly papain cleave tubulin at a small distance from the C-termini. The proportion of internal to terminal cleavages by subtilisin can be modified by buffer composition; this proportion might be dependent on trace divalent cations complexed by EGTA. The terminal cleavage of α-tubulin by subtilisin partially removes the reactivity to anti-α(430–443) antibodies but conserves the region α(415–430); the results also indicate heterogeneity in the cleaved α chain. C-Terminal cleavage of β-tubulin by subtilisin does not remove the reactivity to anti-β(412–431) antibodies, indicating that this region is not substantially cleaved in our system. The approximate cleavage points are indicated in Figure 10. Their exact position cannot be ascertained by the present method; however, the limits to the possible positions are clearly set by the reactivities with the anti-peptide antibodies as well as with the DM1A and DM1B monoclonals. The patterns of subtilisin cleavage and fragment antibody reactivity of purified calf brain tubulin are qualitatively reproduced with microtubule protein (Figure 8B), suggesting that the subtilisin cleavage of unassembled tubulin is essentially independent of the preparation procedure and the presence of MAPs. Preliminary experiments indicate related results with phosphocellulose-purified pig brain tubulin. All this contrasts with the reported removal by subtilisin of C-terminal tubulin fragments of M_r 4000 (Serrano et al., 1984a,b) and may be compatible with the cleavage of 7–15 amino acids from each chain (Sackett et al., 1985). Nevertheless, apparent molecular weight or charge should not be employed to estimate exact cleavage positions, as demonstrated by the chymotrypsin and V8 experiments (Figures 6 and 9, respectively). Maccioni et al. (1986) have reported amino acid analyses of S-tubulin and the small fragments and carboxypeptidase A end group determination of S-tubulin. They concluded that the single cleavage points are α(Glu-417–Phe-418) and β(Glu-407–Phe-408). This is not compatible with our results; the discrepancy could be due to the different tubulin sources, different experimental conditions, and the unusual repetition of glutamic acid residues in the C-terminal regions of tubulin, which makes the chemical determination of cleavage points difficult simply by electrophoretic, end group, and amino acid analyses. Therefore, we prepared the small fragments of subtilisin digestion of purified calf brain tubulin and subjected them to high-performance liquid chromatography, in order to have them sequenced and aligned into the corresponding positions of α- and β-tubulin. However, we found a large number of components, strongly suggesting that calf brain tubulin is cleaved by subtilisin at multiple sites within the small regions determined with the aid of anti-peptide antibodies. There is also the possibility with this and other proteases that differential cleavage of the tubulin isotypes may be adding complexity to the results of the limited proteolysis. Even a single cleavage mode of different β chains (Cleveland & Sullivan, 1985) about position 430 would generate several clearly different small C-terminal fragments instead of a homogeneous product.

We have discussed the individual cleavage patterns of tubulin by different proteases and elucidated conflicting reports in the literature. Taken together, our results show for the first time a unified and clearly defined view of the limited cleavage of tubulin by several proteases of different specificities.

Tubulin Monomers Consist of Three Major Regions Defined by Limited Proteolysis. Let us now consider the relation of the proteolysis patterns to tubulin structure. Proteolytic enzymes preferentially cleave exposed protein segments characterized by high mobility, rather than internal or rigid segments (Neurath, 1980; Fontana et al., 1986). Therefore, the sites of binding of proteases are possibly related to the sites of binding of antibodies (discussed above). The uncertainty associated with the determination of approximate cleavage points of tubulin by the different proteases from the apparent molecular weight of the fragments (shown by the error bars in Figure 11) precludes an unequivocal assignment of each of these points to individual hydrophilicity maxima in Figure 1. An important feature in Figure 11 is that, of the 27 cleavages determined so far, all but a minor one cluster in three zones of the homologous α- and β-tubulin sequences. These zones are statistically defined by the shaded areas in Figure 11 and correspond to the approximate positions 115–165, 260–300, and 420–440 at the C-terminus. These zones correspond, in Figure 1, to epitopes 6–7 (including the flexible glycine cluster), epitope 12, and epitopes 18–19, respectively. Random generation of such a pattern by proteases of different specificities is a very improbable event. Therefore, the result strongly suggests that the tubulin monomers consist of three proteolytically defined large compact regions. Each of these regions, which we shall number 1 (N-terminal), 2 (middle),

and 3 (C-terminal), spans roughly one-third of the chain length. The zones of preferential proteolytic attack should be very accessible segments (loops or hinges) connecting or hanging from these regions. This model, which is indicated on top of Figure 11, does not contradict, but extends, the two-region model of Mandelkow (Mandelkow et al., 1985a; Kirchner & Mandelkow, 1985) in which regions 1 and 2 were not distinguished. Similarly, our model does not preclude subdivision into smaller regions that may be evidenced in further studies. We have systematically examined the quaternary structure of proteolytically nicked tubulin by means of native gel chromatography followed by SDS electrophoresis and have found that under our conditions no large fragments dissociate spontaneously from the protein (J. Morales and J. M. Andreu, unpublished results). This indicates substantial interactions between regions other than the peptide bonds cleaved, in agreement with previous reports (introduction). Which are the spatial relations among the proteolytically defined regions and their role in the binding of ligands? Presently available biochemical results provide a set of limiting conditions,[2] all of which cannot be easily fulfilled simultaneously in their simplest meaning.

What is the exact relationship of the regions defined by limited proteolysis to possible structural domains of tubulin? The three-dimensional structure of tubulin is not known, and the internal structure of the monomers could hardly be appreciated in existing electron microscopy and X-ray diffraction studies (introduction). Very recently, Beese et al. (1987) have obtained an X-ray diffraction model of hydrated microtubules in which three strong electron density regions are detected per tubulin monomer and are interpreted as three structural domains, named A, B, and C; these domains are apparently connected by thinner zones, suggesting a structure that could be quite flexible, so that small changes in the domain arrangement could give rise to polymorphic tubulin assemblies. The correlation of proteolysis to structure need not be as simple and elegant as for the cleavage of the hinge peptide connecting the antigen binding and complement binding parts of antibody molecules (Porter, 1959). However, simple and attractive working models can be made by assigning each of the proteolytically defined regions of tubulin to one of the structural domains. These models are shown solely for the purpose of discussion in Figure 12. It could be easily envisaged how the binding of ligands, such as GTP/GDP by domains 1–2 or colchicine (possibly by a 2–3 cleft or at the intermonomer contact zone) might change the angles between domains in the monomer, the contact between monomers, and therefore the protein assembly. The binding of colchicine, which leads to abnormal tubulin polymerization, was actually proposed to modify the intermonomer interaction geometry (Andreu & Timasheff, 1983). Regarding the GTP/GDP switch of tubulin (microtubule assembly active/inactive), it has been recently shown that GDP–tubulin has an increased ability over GTP–tubulin to form magnesium-induced rings (Howard & Timasheff, 1986). Rings correspond to curved protofilament segments (Mandelkow et al., 1983). The thermodynamic analysis of ring formation by GDP–tubulin in comparison to GTP–tubulin indicates minor differences in the standard free energy change of interdimer association but a large difference in the ring closure step, leading to the hypothesis that GDP–tubulin is in a more favorable conformation for ring closure (Howard & Timasheff, 1986). That is, GDP–tubulin oligomers are assembly inactive because they coil more easily

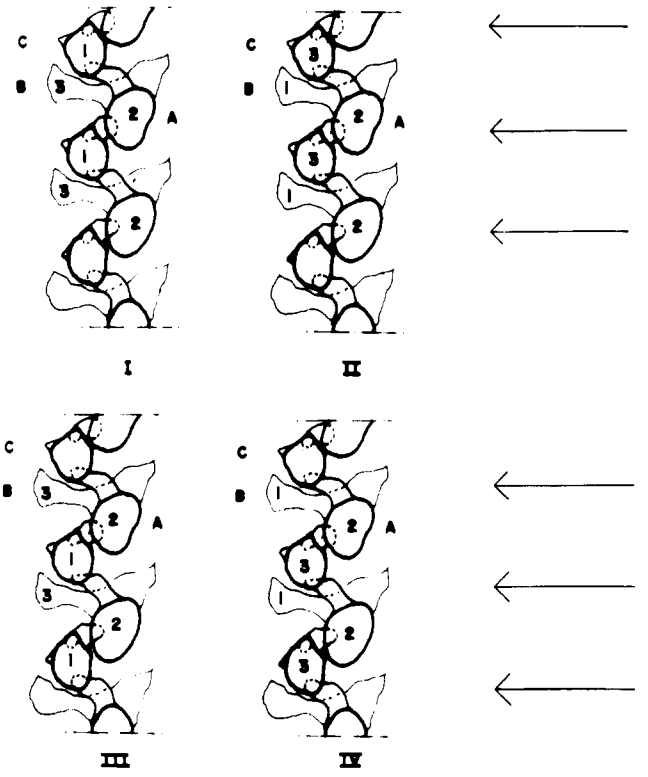

FIGURE 12: Working models of tubulin monomer structure. Each of the proteolytically defined tubulin regions 1–3 (Figure 11) has been assigned to one of the structural domains of the X-ray diffraction microtubule model of Beese et al. (1987). It has been assumed that the peptide chain traverses only once from a domain to the next and that the general structure of the tubulin heterodimer is not drastically different between the soluble and assembled states. A schematic projection of one protofilament is shown, indicating domains C and A and domain B in the back [modified from Figure 5A of Beese et al. (1987)]. The monomer limits are not explicitly reported by Beese et al. (1987). Visual inspection of the less dense zones suggests two possibilities that are indicated by the arrows in models I/II and III/IV respectively. Models I/II can be roughly superimposed, better than models III/IV, to the protofilament image reconstruction of Amos and co-workers, where the monomer limits are clear [see Figure 17 of Amos (1979)]. In models I and II the intramonomer domain connectivity is B–A–C and the intermonomer contacts are of the C–A type; the structural domains corresponding to proteolysis fragments 1, 2, and 3 would be respectively C, A, and B (model I) or B, A, and C (model II). In models III and IV the domain connectivity is C–A–B and the intermonomer contacts are A–C; fragments 1, 2, and 3 would correspond to domains C, A, and B (model III) or B, A, and C (model IV). Application of the set of conditions a–h[2] to these models shows that conditions a, b, d, and e are not openly contradicted by any of the models. Only models II and IV do not contradict condition c and the simultaneous application of conditions c, f, and g. Therefore, II and IV are the best scored models. However, none of the four models satisfies simultaneously conditions c and f–h. More generally, the simultaneous application of conditions c and f–h is incompatible with any model in which the proteolytic fragments correspond to domains arranged along the protofilament, unless their order would be reversed from a monomer to the next one; but this would contradict all the structural studies, which indicate that the polarity of the monomers in a protofilament is the same.

[2] (a) Two cysteine residues of regions 2 and 3 are less than 9 Å apart in the β subunit; (b) the same probably holds for the other two cysteines in regions 1 and 2 of this subunit; (c) region 3 of β is in contact with region 1 + 2 of α in the soluble heterodimer, and therefore the longitudinal contact between heterodimers in the microtubule is between α region 3 and β region 1 + 2; (d) the small C-terminal zones at the end of region 3 participate in the binding of MAPs and are exposed on the outer side of the microtubule wall; (e) the guanine nucleotide binding sites are predicted to be contributed by regions 1 and 2; (f) the zone surrounding Cys-239 of β is important for colchicine binding (the simplest interpretation would be that this zone constitutes part of the colchicine binding site); (g) colchicine binds at a site located in α or less than 18 Å away from this subunit; (h) the colchicine binding site includes region 3 of α. Individual references to a–h are given in the introduction.

than GTP–tubulin oligomers, which could be caused by a flexion of domains 1–2. Contrasting working models I–IV (Figure 12) with the set of relations between tubulin regions in the tubulin heterodimer (conditions a–h)[2] reveals inconsistencies (legend to Figure 12), which strongly suggest one of three possibilities: either the proteolytically defined regions do not correspond to three sequential structural domains, there are marked changes in the position of the domains with respect to each other between soluble tubulin and microtubules, or some of the biochemical conditions[2] applied are incorrect; these are open to further study.

We presently seek to determine the participation of the small zones probed by anti-peptide antibodies, as well as the major regions defined by controlled proteolysis, in microtubule assembly and binding of ligands by tubulin.

Added in Proof

After this paper was submitted, the divergent chicken erythrocyte β-tubulin gene sequence has been reported (Murphy et al., 1987); a zone homologous (with two amino acid differences) to the peptide β(412–431) is found, in agreement with our results (Figure 2D). An antibody to a peptide embracing epitope β7 (Figure 1) has been reported to inhibit GTP incorporation and tubulin polymerization (Hesse et al., 1987). Antibodies to the variable C-terminal extremes of the β-tubulin isotypes have also been raised by use of cloned fusion proteins (Lewis et al., 1987) or synthetic peptides (Lopata & Cleveland, 1987). Determinants for the monoclonal antibody TU-01 have been mapped in positions α(65–79) (Grimm et al., 1987).

Acknowledgments

We thank J. Morales for technical assistance, Dr. L. Utrilla for the immunofluorescences of Figure 3E,F, F. Postiguillo for Figure 12, and Dr. E. Fernandez for the use of her photomicroscope (Figures 3A–D and 5). We are indebted to Dr. R. Manso for the gift of calf brain microtubule protein, Dr. V. Peyrot for phosphocellulose purified pig brain tubulin, and Dr. T. J. Fitzgerald for the bicyclic colchicine analogue.

References

Amit, A. G., Mariuzza, R. A., Phillips, S. E. V., & Poljak, R. (1986) *Science (Washington, D.C.) 233*, 747–754.

Amos, L. A. (1979) in *Microtubules* (Roberts, K., & Hyams, J. S., Eds.) pp 1–64, Academic, New York.

Andreu, D., de la Viña, S., & Andreu, J. M. (1988) *Int. J. Pept. Protein* Res. (in press).

Andreu, J. M., & Timasheff, S. N. (1982) *Biochemistry 21*, 6465–6476.

Andreu, J. M., & Timasheff, S. N. (1983) *Biochemistry 22*, 1556–1566.

Andreu, J. M., de la Torre, J., & Carrascosa, J. L. (1986) *Biochemistry 25*, 5230–5239.

Avila, J., Serrano, L., & Maccioni R. M. (1987) *Mol. Cell. Biochem. 73*, 29–36.

Beese, L., Stubbs, G., & Cohen, C. (1987) *J. Mol. Biol. 194*, 257–264.

Blose, S. H., Meltzer, D. I., & Feramisco, J. R. (1984) *J. Cell Biol. 98*, 847–858.

Breitling, F., & Little, M. (1986) *J. Mol. Biol. 189*, 367–370.

Chanock, R. M., & Sabin, A. B. (1953) *J. Immunol. 70*, 271–285.

Chou, P. Y., & Fasman, G. D. (1978) *Adv. Enzymol. Relat. Areas Mol. Biol. 47*, 45–148.

Clayton, L., & Lloyd, C. W. (1984) *Eur.* J. *Cell Biol. 34*, 248–253.

Cleveland, D. W., & Sullivan, K. F. (1985) *Annu. Rev. Biochem. 54*, 331–365.

Diez, J. C., Avila, J., Nieto, J. M., & Andreu, J. M. (1987) *Cell Motil. Cytoskeleton 7*, 178–187.

Eisenberg, D. (1984) *Annu. Rev. Biochem. 53*, 595–623.

Finer-Moore, J., & Stroud, R. M. (1984) *Proc. Natl. Acad. Sci. U.S.A. 81*, 155–159.

Fontana, A., Fassina, G., Vita, C., Dalzopo, D., Zamai, M., & Zambonin, M. (1986) *Biochemistry 25*, 1847–1851.

Garnier, J., Osguthorpe, D. J., & Robson, B. (1978) *J. Mol. Biol. 120*, 97–120.

Grimm, M., Breitling, F., & Little, M. (1987) *Biochim. Biophys. Acta 914*, 83–88.

Gundersen, G. G., Kalnoski, M. H., & Bulinski, J. C. (1984) *Cell (Cambridge, Mass.) 36*, 779–789.

Gundersen, G. G., Khawaja, S., & Bulinski, J. C. (1987) *J. Cell Biol. 105*, 251–264.

Hesse, J., Thierauf, M., & Ponstingl, H. (1987) *J. Biol. Chem. 262*, 15472–15475.

Hopp, T. P., & Woods, K. R. (1981) *Proc. Natl. Acad. Sci. U.S.A. 78*, 3824–3828.

Howard, W. D., & Timasheff, S. N. (1986) *Biochemistry 25*, 8292–8300.

Karplus, P. A., & Schultz, G. E. (1985) *Naturwissenschaften 72*, 212–213.

Kilmartin, J. V., Wright, B., & Milstein, C. (1982) *J. Cell Biol. 93*, 576–582.

Kirchner, K., & Mandelkow, E. M. (1985) *EMBO J. 4*, 2397–2402.

Krauhs, E., Little, M., Kempf, T., Hofer-Warbinek, R., Ade, W., & Ponstingl, H. (1981) *Proc. Natl. Acad. Sci. U.S.A. 78*, 4156–4160.

Kyte, J., & Doolittle, R. F. (1982) *J. Mol. Biol. 157*, 105–132.

Lee, J. C. (1981) *Methods Cell Biol. 24*, 9–30.

Lee, J. C., Frigon, R. P., & Timasheff, S. N. (1973) *J. Biol. Chem. 248*, 7253–7262.

Lewis, S. A., Gu, W., & Cowan, N. J. (1987) *Cell (Cambridge, Mass.) 49*, 539–548.

Little, M., & Ludueña, R. F. (1985) *EMBO J. 4*, 51–56.

Little, M., & Ludueña, R. F. (1987) *Biochim. Biophys. Acta 912*, 28–33.

Lopata, M., & Cleveland, D. W. (1987) *J. Cell Biol. 105*, 1707–1720.

Maccioni, R. B., & Seeds, N. W. (1983) *Biochemistry 22*, 1567–1572.

Maccioni, R. B., Serrano, L., Avila, J., & Cann, J. R. (1986) *Eur. J. Biochem. 156*, 375–381.

Mandelkow, E., Thomas, J., & Cohen, C. (1977) *Proc. Natl. Acad. Sci. U.S.A. 73*, 3370–3374.

Mandelkow, E., Mandelkow, E. M., & Bordas, J. (1983) *J. Mol. Biol. 167*, 179–186.

Mandelkow, E. M., & Mandelkow, E. (1985) *J. Mol. Biol. 181*, 123–135.

Mandelkow, E. M., Herrmann, M., & Ruhl, U. (1985a) *J. Mol. Biol. 185*, 311–327.

Mandelkow, E. M., Kirchner, K., & Mandelkow, E. (1985b) in *Microtubules and Microtubule Inhibitors* (DeBrabander, M., & DeMey, J., Eds.) pp 31–47, Elsevier, Amsterdam.

Manso-Martinez, R., Palomares, R., & Pariente, F. (1984) *Arch. Biochem. Biophys. 235*, 196–203.

Merrifield, B. (1963) *J. Am. Chem. Soc. 85*, 2149–2156.

Morejohn, L. C., Bureau, T. E., Tocchi, L. P., & Fosket, D. E. (1984) *Proc. Natl. Acad. Sci. U.S.A. 81*, 1440–1444.

Murphy, D. B., & Wallis, K. T. (1983) *J. Biol. Chem. 258*, 7870–7875.

Murphy, D. B., Wallis, K. T., Machlin, P. S., Ratrie, H., III, & Cleveland, D. W. (1987) *J. Biol. Chem. 262*, 14305–14312.
Na, G. C., & Timasheff, S. N. (1982) *Methods Enzymol. 85*, 393–408.
Neff, N. F., Thomas, J. H., Grisafi, P., & Botstein, D. (1983) *Cell (Cambridge, Mass.) 33*, 211–219.
Neurath, H. (1980) in *Protein Folding* (Jaenicke, R., Ed.) pp 501–524, Elsevier/North-Holland, Amsterdam and New York.
Piperno, G., & Fuller, M. T. (1985) *J. Cell Biol. 101*, 2085–2094.
Ponstingl, H., Little, M., Krauhs, E., & Kempf, T. (1979) *Nature (London) 282*, 423–424.
Ponstingl, H., Krauhs, E., Little, M., & Kempf, T. (1981) *Proc. Natl. Acad. Sci. U.S.A. 78*, 2757–2761.
Porter, R. R. (1959) *Biochem. J. 73*, 119–127.
Prakash, V., & Timasheff, S. N. (1982) *J. Mol. Biol. 160*, 499–515.
Raugi, G. J., Mumby, S. M., Abbot-Brown, D., & Bornstein, P. (1982) *J. Cell Biol. 95*, 351–354.
Ringel, I., & Sternlicht, H. (1984) *Biochemistry 23*, 5644–5653.
Roach, M. C., Bane, S., & Ludueña, R. F. (1985) *J. Biol. Chem. 260*, 3015–3023.
Rose, G. D., Gierasch, L. M., & Smith, J. A. (1985) *Adv. Protein Chem. 37*, 1–109.
Sackett, D. L., & Wolff, J. (1986) *J. Biol. Chem. 261*, 9070–9076.
Sackett, D. L., Bhattacharyya, B., & Wolff, J. (1985) *J. Biol. Chem. 260*, 43–45.
Serrano, L., de la Torre, J., Maccioni, R. B., & Avila, J. (1984a) *Proc. Natl. Acad. Sci. U.S.A. 81*, 5989–5993.
Serrano, L., Avila, J., & Maccioni, R. B. (1984b) *Biochemistry 23*, 4675–4681.
Serrano, L., Valencia, A., Caballero, R., & Avila, J. (1986a) *J. Biol. Chem. 261*, 7076–7081.
Serrano, L., Wandosell, F., & Avila, J. (1986b) *Anal. Biochem. 159*, 253–259.
Soifer, D., Ed. (1986) *Ann. N.Y. Acad. Sci. 466*.
Sternlicht, H., Yaffe, M. B., & Farr, g. W. (1987) *FEBS Lett. 214*, 226–235.
Valenzuela, P., Quiroga, M., Zaldivar, J., Rutter, W. J., Kirschner, M. W., & Cleveland, D. W. (1981) *Nature (London) 289*, 650–655.
Wehland, J., Willingham, M. C., & Sandoval, I. V. (1983) *J. Cell Biol. 97*, 1467–1475.
Wehland, J., Schroeder, H. C., & Weber, K. (1984) *EMBO J. 3*, 1295–1300.
Welling, G. W., Weifer, W. J., van der Zee, R., & Welling-Wester, S. (1985) *FEBS Lett. 188*, 215–218.
Wick, S. M., Seagull, R. W., Osborn, M., Weber, K., & Gunning, B. E. S. (1981) *J. Cell Biol. 89*, 685–690.
Williams, R. F., Mumford, C. L., Williams, G. A., Floyd, L. J., Aivaliotis, M. J., Martinez, R. A., Robinson, A. K., & Barnes, L. D. (1985) *J. Biol. Chem. 260*, 13794–13802.
Youngbloom, J., Schloss, J. A., & Silflow, C. D. (1984) *Mol. Cell. Biol. 4*, 2686–2696.

Manganese Peroxidase from the Basidiomycete *Phanerochaete chrysosporium*: Spectral Characterization of the Oxidized States and the Catalytic Cycle†

Hiroyuki Wariishi, Lakshmi Akileswaran, and Michael H. Gold*
Department of Chemical and Biological Sciences, Oregon Graduate Center, Beaverton, Oregon 97006-1999
Received January 15, 1988; Revised Manuscript Received March 10, 1988

ABSTRACT: Manganese peroxidase (MnP), an extracellular heme enzyme from the lignin-degrading fungus *Phanerochaete chrysosporium*, catalyzes the Mn(II)-dependent oxidation of a variety of phenols. Herein, we spectroscopically characterize the oxidized states of MnP compounds I, II, and III and clarify the role of Mn in the catalytic cycle of the enzyme. Addition of 1 equiv of H_2O_2 to the native ferric enzyme yields compound I, characterized by absorption maxima at 407, 558, 605, and 650 nm. Addition of 2 or 250 equiv of H_2O_2 to the native enzyme yields compound II or III, respectively, identified by absorption maxima at 420, 528, and 555 nm or at 417, 545, and 579 nm, respectively. These characteristics are very similar to those of horseradish peroxidase (HRP) and lignin peroxidase (LiP) compounds I, II, and III. Addition of 1 equiv of either Mn(II), ferrocyanide, or a variety of phenols to MnP compound I rapidly reduces it to MnP compound II. In contrast, only Mn(II) or ferrocyanide, added at a concentration of 1 equiv, reduces compound II. The Mn(III) produced by the enzymic oxidation of Mn(II) oxidizes the terminal phenolic substrates. This indicates that compounds I and II of MnP contain 2 and 1 oxidizing equiv, respectively, over the native ferric resting enzyme and that the catalytic cycle of the enzyme follows the path native enzyme → compound I → compound II → native enzyme. In addition, these results indicate that Mn(II) serves as an obligatory substrate for MnP compound II, allowing the enzyme to complete its catalytic cycle. Finally, the Mn(II)/Mn(III) redox couple enables the enzyme to rapidly oxidize the terminal phenolic substrates.

Lignin is a complex, optically inactive, and random phenylpropanoid polymer that comprises 20–30% of woody plants (Sarkanen, 1971). Since the biodegradation of cellulose is retarded by the presence of lignin (Crawford, 1981), the catabolism and potential utilization of this polymer are of enormous significance. White rot basidiomycetes are primarily responsible for the initiation of the decomposition of lignin in wood (Crawford, 1981). Recent studies have shown that when cultured under ligninolytic conditions, the white rot basi-

† This work was supported by Grants DMB 86-07279 from the National Science Foundation and FG06-86-ER-13550 from the U.S. Department of Energy.
* To whom correspondence should be addressed.

0006-2960/88/0427-5365$01.50/0